9210 *Macromolecules* **2010**, *43*, 9210–9214
DOI: 10.1021/ma1019895

Macromolecules
NOTE

A Trajectory-Extending Kinetic Monte Carlo (TEKMC) Method for Estimating Penetrant Diffusion Coefficients in Molecular Dynamics Simulations of Glassy Polymers

S. Neyertz* and D. Brown*

LMOPS-UMR CNRS 5041, University of Savoie, Bât. IUT, Savoie Technolac, 73376 Le Bourget-du-Lac Cedex, France

Received August 27, 2010; Revised Manuscript Received September 28, 2010

1. Introduction

Molecular dynamics (MD)[1] simulation techniques are increasingly used to predict transport rates of gases in bulk polymers.[2] If $\boldsymbol{r}_i(t)$ is the position of penetrant atom i at time t, the most common way of evaluating the gas self-diffusion coefficient D_{gas} involves the calculation of mean-square displacements at different times t of the trajectories, MSDs = $\langle(\boldsymbol{r}_i(t + t_0) - \boldsymbol{r}_i(t_0))^2\rangle$, which are averaged over all penetrant molecules and all possible time origins t_0 of the production runs. The MSDs can then be used to evaluate D_{gas} using Einstein's equation (eq 1):[3]

$$D_{gas} = \lim_{t \to \infty} \frac{1}{6t}\langle(\mathbf{r}_i(t+t_0) - \mathbf{r}_i(t_0))^2\rangle \qquad (1)$$

However, eq 1 assumes that the gas molecules follow a random walk. In dense polymers, where penetrant motion is strongly affected by the immediate environment, this condition is only really valid within the framework of a long-time Fickian diffusive limit, i.e., when the MSDs are proportional to t. In the intervening time, with the exception of a short-time ballistic regime at the very start, the MSD curves are usually proportional to t^n with $n < 1$, which characterizes the anomalous diffusion regime.[3−5] In spite of the constant increase in computer power, fully atomistic MD simulations can still only realistically probe time scales of a few to tens of nanoseconds. Using eq 1, this means that only diffusivities exceeding $\sim 10^{-6}$ cm^2 s^{-1},[2] i.e., when the motion of the penetrant is fast enough for its MSD to go from being anomalous to Fickian (characterized by a slope of one on the log(MSD)−log(t) plots), can be reliably measured within the time scale of the MD simulation. However, diffusion of many common gases is slower, ranging typically from 10^{-7} to 10^{-8} cm^2 s^{-1} in glassy polymer matrices.[6,7]

In this work, we present a variant of the Kinetic Monte Carlo (KMC) approach,[2,5,8−14] which is based on a relatively straightforward analysis of the *actual trajectories of gas molecules in the polymer*. Providing that enough of the percolating paths through the polymer system are revealed during the limited atomistic MD simulation, we propagate the penetrant trajectories further in time based on the actual existing MD runs in order to obtain MSDs on longer time scales. As such, we refer to it as "trajectory-extending kinetic Monte Carlo" or "TEKMC". Since it is only valid in regimes where penetrant concentrations and mobilities are high enough to probe a sufficient part of the available trajectories in polymer−penetrant MD simulations, it is important to note that this method is not intended to replace the sophisticated approaches that obtain the penetrant diffusion coefficient in the infinite dilution limit from an analysis of the pure polymer system.[2,5,8−14] However, there are experimentally accessible pressure regimes for soluble and mobile penetrants, for which TEKMC can be used to obtain reliable estimates of the extended MSDs. The application of TEKMC has been recently briefly introduced for CO_2 in fluorinated polyimides,[15] but we give here further details of the technique and show that it can be used for other small penetrants such as H_2O, O_2, and N_2 in glassy polymer matrices.

*Corresponding authors. E-mail: (S.N.) sylvie.neyertz@univ-savoie.fr; (D.B.) david.brown@univ-savoie.fr.

2. The TEKMC Method

TEKMC is a crude and fairly simple method to extend the time range over which the penetrant MSDs in polymer systems can be evaluated in fully periodic systems. It requires as input a set of stored configurations from a MD simulation of the polymer−penetrant system over a time interval in which the penetrant molecules explore a significant part of the periodic system. Motion of small penetrant molecules in glassy dense matrices is known to be based on combinations of oscillations within available free volumes and occasional jumping events by hopping between different voids, which are made possible by the temporary opening of channels within the polymer matrix.[3,5,11] Figure 1 shows the trajectories taken by penetrants such as H_2O and CO_2 in some glassy polyimide matrices over the nanosecond time scale of MD simulations. For clarity, the trajectories have been "folded back" into the primary MD box; periodic boundary conditions being applied in all three dimensions. Although the volume accessible to the penetrants at any one time varies slightly depending on the natural fluctuations of the polymer matrix, it remains correlated on the MD time scale. It is clear from Figure 1 that the penetrants are restricted to certain zones of the MD box by the presence of the polymer, but that there is also a sufficient amount of space accessible to allow them to diffuse through "channels" that form an interconnecting and percolating network.

Providing that the penetrant molecules are able to reveal this interconnecting network of channels over the MD simulation, the first stage of the procedure can be described as follows. It is necessary to choose the time interval τ between the configurations of the original run that will be analyzed. For example, if the MD configurations were originally stored at 10 ps intervals, one can either choose τ = 10 ps, which is the simplest alternative, or any multiple of 10 ps for τ. Once τ has been set, the actual trajectories are assigned to subcells of the primary MD box based on the folded positions of the penetrant central atom or center-of-mass. This is performed using the set of scaled coordinates $\boldsymbol{s}_i = \mathbf{h}^{-1}\boldsymbol{r}_i$ where the matrix $\mathbf{h} = \{\mathbf{a}, \mathbf{b}, \mathbf{c}\}$ is defined from the basis vectors of

 Published on Web 10/12/2010

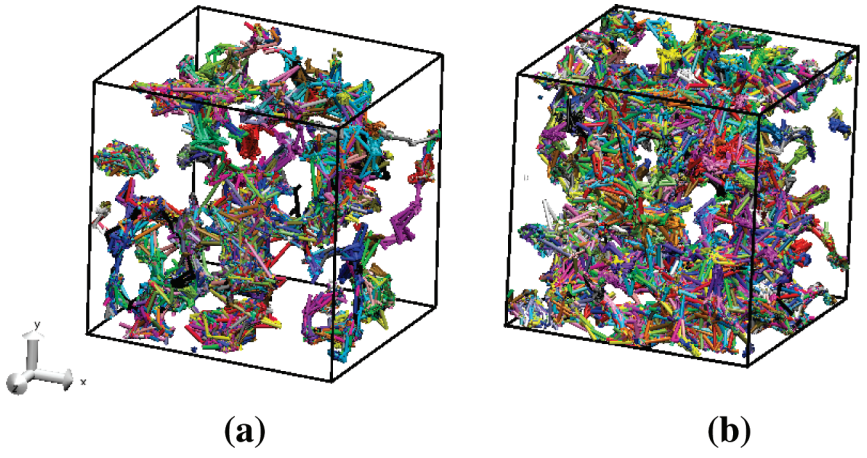

Figure 1. Typical penetrant trajectories in ~10000-atom amorphous glassy polymers in nanosecond-long MD simulations performed with the MD code of the *gmq* package[16] and displayed with the VMD 1.8.2 software.[17] (a) A PMDA−ODA+3.4 wt %H_2O 5000 ps simulation at 373 K. (b) A 6FDA−6FpDA+15 wt %CO_2 5000 ps simulation at 308 K. The volumes of both boxes are ≈51 Å^3 and the technical details of the simulations are given in refs 15, 18, and 19. Separate colors are used to trace the trajectories of different molecules. Configurations were stored at 10 ps intervals so each straight segment of the trajectories corresponds to this time interval.

the MD box. All subcells are of the same size and shape and the resolution of the subcell grid is set by the parameter D_{grid} which has to be optimized (see later). For each subcell that has been visited by a penetrant molecule, a record is kept of the identity of all subcells that are moved to at subsequent steps and the number of times that they are moved to. We point out that no restrictions are placed on which subcells are potentially connected. If the penetrant remains in the same subcell between subsequent analyzed configurations, this too is also recorded. This procedure allows us to define a probability matrix for jumps to occur between any two subcells based on the actual analyzed configurations of the MD run. It is also important that the connectivity of the visited cells is examined in order to check that they are mostly in one interconnected pathway. As there will always be penetrants that remain in non-percolating channels over the time scale of such MD simulations, we arbitrarily set a minimum tolerance of 90% for the connectivity (i.e., at least 90% of the visited cells must belong to the same percolating path). This is tantamount to a maximum error of 10% on the simulated D, which is smaller than the large amount of scatter found in the experimental D for the same polymer and penetrant.[15] However, it is better to aim for lower errors and indeed, for the 5000 ps MD simulations of H_2O and CO_2 in polyimides displayed in Figure 1, the visited cells that belong to a single cluster amount to >98%. Testing for the connectivity is fundamental since the resulting D will tend to zero if the channels are not linked, which is clearly an artifact. In this case, the basic MD simulation should be extended or alternatively, a technique other than TEKMC[2,5,8−14] should be used.

The second stage of the procedure is a separate kinetic Monte Carlo phase. A number of walks, typically of the order of 5000, are carried out separately. Each one is initiated from a randomly selected subcell among those that have been visited. At each step of a walk, a subcell to jump to is selected with a probability corresponding to that found in the first phase from the list of subcells that can be reached from the current subcell. Jumps between cells are made using the nearest image convention so that the walks will be continuous in space. In order to avoid the walks becoming trapped, the probability matrix is artificially symmetrized. This is equivalent to enforcing detailed balance, i.e. the flux of particles from cell I to J is the same, on average, as those from cell J to cell I. In terms of probabilities of being in a particular cell and the rate constants for the jumps between cells, this can be expressed as $p_I k_{IJ} = p_J k_{JI}$. As far as interactions between penetrants are concerned, the advantage of the TEKMC method is that the jump probability matrix is constructed from the actual penetrant trajectories in a system *where many penetrants are present*. The probability matrix thus implicitly takes into account all issues related to penetrant−penetrant interactions, and the TEKMC walks are subject to this multipenetrant constructed probability matrix.

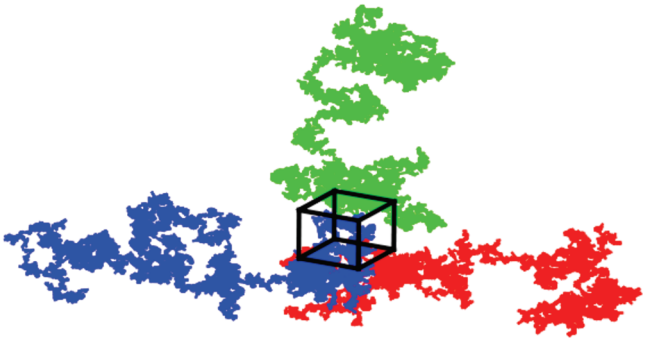

Figure 2. Two-dimensional projection of three different TEKMC walks generated from the 6FDA−6FpDA + 15%CO_2 5000 ps MD simulation at 308 K shown in Figure 1b and extended up to 500000 ps (volume of the primary box ≈ 51 Å^3).

As the elemental steps of the walks are determined by the measured jump probability matrix, it would be misleading to refer to them as "random" walks. The analogy with a true random walk can only be made at long times, when there is no correlation between the direction of subsequent steps. Examples of three TEKMC walks, in the case of a 6FDA−6FpDA + 15 wt % CO_2 5000 ps simulation (Figure 1b), are shown in Figure 2. Each walk starts from the primary MD cell and is colored differently. The walk trajectories were generated over 500000 ps with a step of 10 ps between the KMC moves. While this step has to be necessarily equal to the τ interval between the analyzed configurations of the original MD run, the generation of the walks is relatively rapid. The efficiency of the method as a whole can be significantly improved by reducing the resolution in the subsequent calculation of the MSDs for the walks. For example, in TEKMC runs extended up to 10 million ps, the resolution of the associated MSDs could be easily set to 10000 ps.

The results are found to be sensitive to the choice of both the time-interval between the analyzed MD configurations, τ, and the grid resolution, D_{grid}. τ should not be too short, e.g., of the same order than the MD 10^{-15} s time step, since it will not be sufficient to allow for jumps between cavities to occur and it will be very

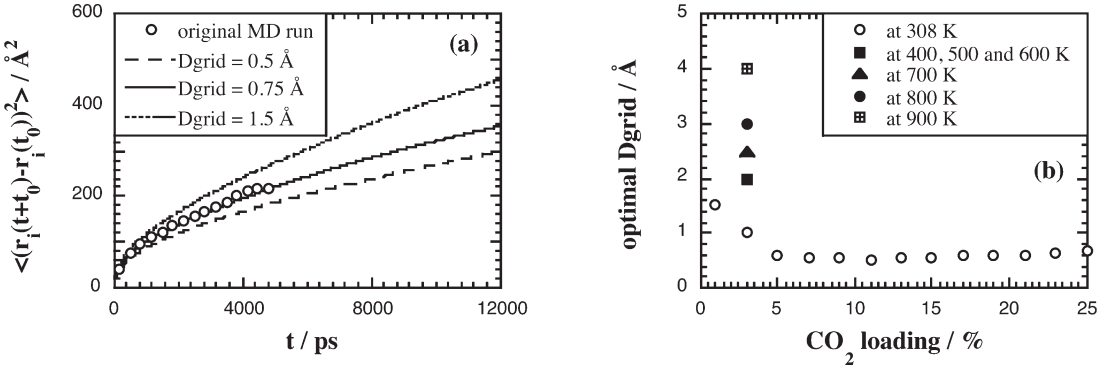

Figure 3. (a) H_2O MSDs vs time t in PMDA−ODA + 3.4% H_2O obtained either directly from the actual 5000 ps MD simulation (circles) or from TEKMC (lines) with $\tau = 10$ ps and three different grid resolutions, $D_{grid} = 0.5$, 0.75, and 1.5 Å. (b) The optimal D_{grid} parameter for CO_2 in the 6FDA−6FpDA polyimide with $\tau = 10$ ps as a function of CO_2 loading and temperature.

inefficient in the walk generation phase. τ should not be too long either as penetrants would appear to "jump" distances which approach half the size of the MD cell, i.e., the maximum distance for which the direction of a jump can be identified uniquely for just those subcells in the primary MD box. However, between these extremes, there is a broad region of possible values for τ. As far as D_{grid} is concerned, it should reflect to some extent the natural fluctuations a penetrant molecule will have within a cavity. If D_{grid} is too small, it will lead to an underestimation of the connectivity between the different trajectories taken by the penetrants and thus to slower diffusion. On the other hand, too coarse a grid will overestimate the connectivity and lead to faster diffusion. Among τ and D_{grid}, either one can be varied in order to perform the optimization, and thus there are a number of "optimum" (τ, D_{grid}) combinations which, along with their associated matrices of jump probabilities, are equivalent in terms of the TEKMC-predicted limiting MSDs. In practice, as noted above, the simplest is to set τ to the typical time-interval used between storing the configurations in the MD simulation, i.e., usually of the order of 10 ps, and then optimize D_{grid}.

As illustrated by Figure 3a for H_2O in PMDA−ODA and τ = 10 ps, D_{grid} can be easily tuned in TEKMC by first reproducing the penetrant MSDs over the time-interval of the original MD runs. For this particular system, the optimal value for D_{grid} is 0.75 Å. In general, we find subcell grid resolutions for gas molecules in different glassy polyimides with $\tau = 10$ ps to be typically of the order of 0.3−0.9 Å in the 300−400 K interval, with a small trend for the larger D_{grid} to be associated with those polymers with faster penetrant diffusion. As far as a specific polymer is concerned, the variation of the optimal D_{grid} parameters obtained at 308 K (white circles) for different CO_2 loadings, ranging from 1% to 25% in the 6FDA−6FpDA polyimide is illustrated in Figure 3b. At a given temperature and fixed τ, D_{grid} remains fairly constant as a function of penetrant loading, with the exception of the very low loadings which suffer from a limited sampling of the void volume in the original MD simulations. On the other hand, the optimal D_{grid} is correlated to the temperature at fixed τ. This is shown in Figure 3b by the 3%CO_2 system, which was also studied as a function of temperature in the 400−900 K range (black symbols and squares). The choice of a low-loading system for this stage was justified by the well-known decrease in solubility as temperature increases,[20] and it was checked that the diffusion mechanism in the temperature range under study was still that of the low-temperature hopping regime.[15] Figure 3b shows that D_{grid} increases with temperature at fixed τ, in keeping with the increased mobility of the penetrants at higher temperatures. However, the interdependence between τ and D_{grid} makes it difficult to discuss the "physical meaning" of either of these parameters in isolation.

The validity of TEKMC should first be tested in systems where D_{gas} can be directly obtained from eq 1. Although this would require more than a year in CPU costs for ~10000-atom models at 308 K with the full potential, two additional MD simulations based on 6FDA−6FpDA and 6FDA−6FmDA fluorinated polyimides with 15%CO_2[15] were carried out up to 100 ns. In these test systems, referred to hereafter as "PDA 15%" and "MDA 15%", the partial charges were removed, a short-range repulsive WCA form was used for the van der Waals interactions and the simulations were run under constant-volume conditions. Despite these changes to the potential, the diffusion mechanism remains that of the hopping-type, but the required CPU times per time step are significantly reduced. However, we emphasize that the changes in the potential were made simply to provide test systems for which we could perform long simulations in a reasonable time and not as an attempt to obtain approximate results for the full-potential systems.

In these test systems, TEKMC jump probabilities between subcells were obtained from just the first 5 ns of the simulations and the D_{grid} parameter optimized to reproduce the actual first 5 ns of the CO_2 mean square displacements (Figure 4a). The optimal D_{grid} at 308 K was found to be 0.6 Å for PDA 15% and 0.47 Å for MDA 15%. The TEKMC method was then used to predict the behavior of the CO_2 MSDs out to the 100 ns of these MD simulations, without making any further adjustments (Figure 4b for PDA 15% and Figure 4c for MDA 15%). The agreement between the TEKMC-predicted MSDs and the actual MSDs obtained through MD is clearly very good. A similar test was carried out on the higher-temperature 6FDA−6FpDA + 3% CO_2 system at 600 K with the full interactions switched on,[15] for which the crossover from anomalous to Fickian diffusion occurs around 2000 ps. Figure 4d displays the penetrant MSD/6t vs t curve of the MD production run at 600 K (black squares) along with the corresponding TEKMC-generated curves using different time-intervals of the original MD simulation. As can be seen, trajectories can be propagated further in time with TEKMC in all these cases, providing that the appropriate optimal D_{grid} parameter (given in parentheses in Figure 4d) is used. It is obvious that the length of the original MD run at the basis of the probability matrix for the jumps to occur in TEKMC is likely to affect D_{grid}. However, shorter simulations are tantamount to having a small number of penetrants (see low loadings in Figure 3b); i.e., in both cases, the limited resolution of the available paths in the original MD simulations can be partly compensated for by increasing D_{grid}. TEKMC is thus clearly able to reproduce the trajectories for systems which have reached the Fickian regime under the MD time scale (lines and circles in Figure 4b) and to predict the right D_{gas} even if the length of the original MD simulation used to define the probability matrix is not enough to see the actual

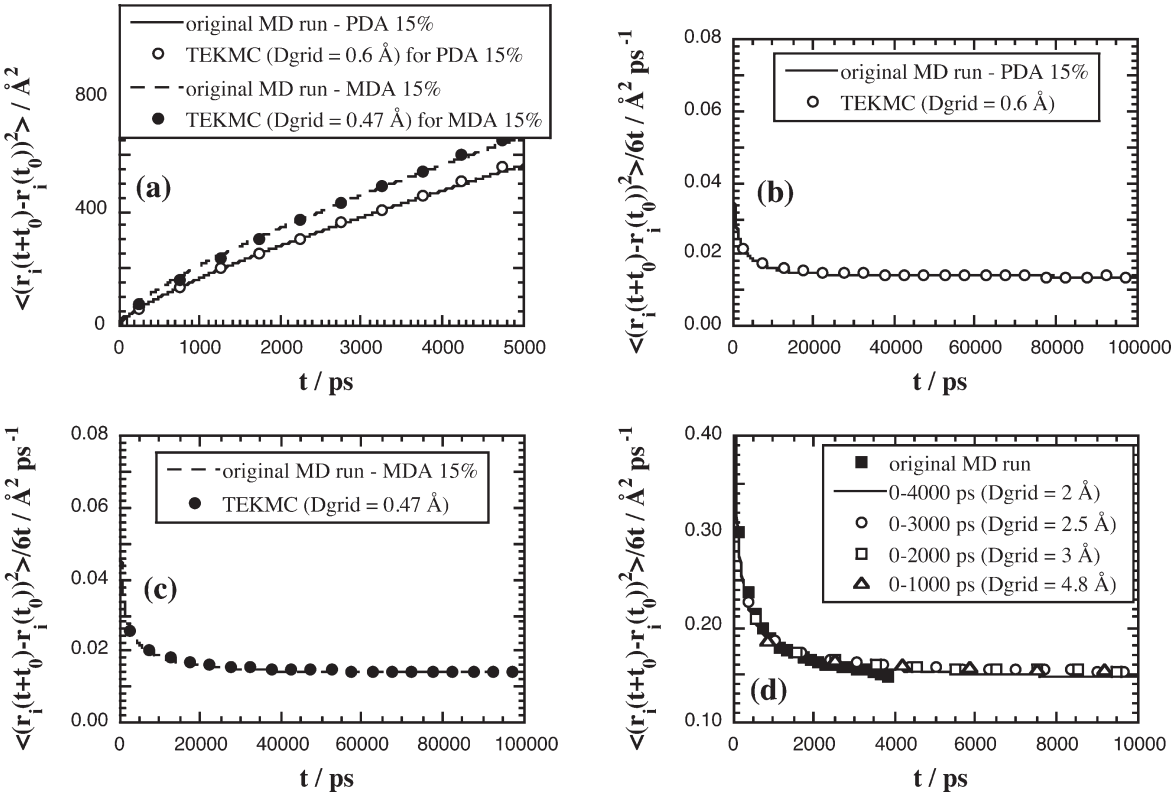

Figure 4. (a) CO_2 MSDs vs time t over the first 5 ns of the PDA 15% and the MDA 15% simulations based on fluorinated polyimides with 15% CO_2 and with a modified potential (see text for details). (b) CO_2 MSD/6t vs t curves in PDA 15% extended up to 100 ns. (c) Same as part b but for MDA 15%. (d) CO_2 MSD/6t vs t curves in 6FDA−6FpDA + 3% CO_2 at 600 K with the full potential. The actual MD data are displayed with black squares. The other curves have all been generated with TEKMC by using as a reference different time-intervals of the original MD run. τ = 10 ps and the optimal D_{grid} is written in parentheses for each case.

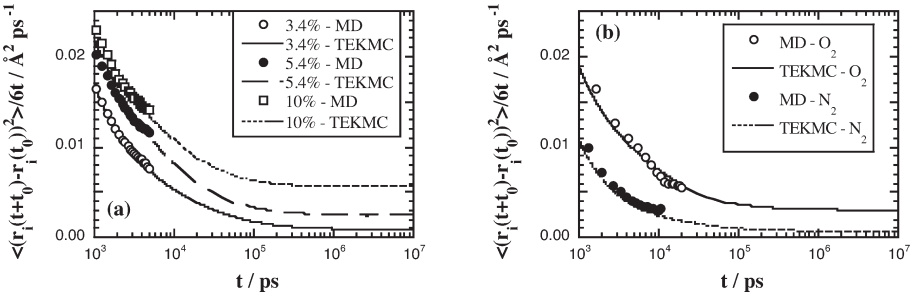

Figure 5. (a) H_2O MSD/6t vs t curves in PMDA−ODA at 373 K obtained either from their actual 5000 ps MD runs (symbols) or from TEKMC (lines). The percentages refer to the H_2O loading and the D_{grid} used were all ~0.7 Å. Note that the x-axis is displayed on a logarithmic scale. (b) O_2 and N_2 MSD/6t vs t curves in 6FDA−6FpDA at 300 K. The legend is the same as in part a and the D_{grid} are 0.4 Å for O_2 and 0.3 Å for N_2. The potentials used are described in refs 24−27, and τ = 10 ps for all cases.

transition from anomalous to Fickian diffusion (white squares and triangles in Figure 4b). For the specific case of CO_2 in fluorinated polyimides, TEKMC results at 308 K, which compared well with experimental evidence, were also found to be in good agreement with an Arrhenius extrapolation of the higher temperatures D_{CO_2} obtained from the direct application of eq 1.[15] This in itself is an additional validation of the TEKMC method.

The efficiency of TEKMC at extending the penetrant trajectories for other systems where the Fickian regime has not been reached with MD is illustrated in Figure 5a for H_2O in PMDA−ODA and in Figure 5b for O_2 and N_2 in 6FDA−6FpDA. The MSDs are correctly reproduced for the initial 5000−20000 ps time scales of the various MD productions runs and the TEKMC-generated walks have been extended up to 10^7 ps. In Figure 5a, the D_{H_2O} are found to be respectively (9, 25, 57) × 10^{-8} cm^2 s^{-1} for the (3.4, 5.4, 10)% wt H_2O loadings respectively, i.e. close to the experimental value of 11 × 10^{-8} cm^2 s^{-1} extrapolated to 373 K for 4.8 wt %.[21] In such systems, an agreement within a factor 2−3 for the diffusion coefficient is usually considered as very good,[3] taking into account both the simplified nature of the modeling and the many different experimental factors that affect permeation in glassy systems. In the case of O_2 in 6FDA−6FpDA (Figure 5b), the TEKMC-extrapolated value of 3 × 10^{-7} cm^2 s^{-1} is also close to the experimental D_{O_2} of 1 × 10^{-7} cm^2 s^{-1}.[22,23] The same applies to N_2 in 6FDA−6FpDA (Figure 5b), where the TEKMC-extrapolated value of 7 × 10^{-8} cm^2 s^{-1} compares well to the experimental D_{N_2} of 4 × 10^{-8} cm^2 s^{-1}.[22,23] In all cases under study, TEKMC is thus clearly able to predict diffusivities which are under 10^{-6} cm^2 s^{-1} and belong to the 10^{-7}−10^{-8} cm^2 s^{-1} range. This provides an estimation of what can be attempted using reasonable time for the original MD simulations.

3. Conclusion

A simple and efficient "trajectory-extending kinetic Monte Carlo" (TEKMC) method, which is based on an analysis of the actual MD trajectories of gas molecules in a polymer matrix, has been presented. It can be applied to various small penetrants, such as CO_2, H_2O, O_2, or N_2, as long as a sufficient amount of their percolating paths through the polymer system are revealed in the limited duration of the atomistic MD simulation. At a first stage, all the penetrant positions over the analyzed configurations (separated by a time-interval τ, which we recommend to be the MD configurations storage interval, i.e. typically 10 ps) are assigned to subcells of the primary MD box. This leads to a probability matrix for jumps to occur between specific subcells. At a second stage, separate kinetic Monte Carlo walks are carried out on the grid of visited subcells with each walk starting from a randomly selected subcell. At each step of a walk, a subcell to jump to is selected with a probability corresponding to that found in the first phase. As the probability matrix is generated from an actual multipenetrant MD simulation, all issues concerning penetrant−penetrant interactions are implicitly taken into account. Providing that τ is set to a suitable value and that the resolution of the subcell grid is optimized with respect to the MSDs of the original MD runs, TEKMC is found to be able to both reproduce the trajectories for systems which have reached the Fickian regime and predict D_{gas} for systems where this regime is difficult to reach with MD simulations. Penetrant MSDs can be obtained over time scales which are at least 3 orders of magnitude longer than the original MD runs at negligible costs in terms of computing time. However, it should be noted that TEKMC is only appropriate at intermediate to high concentrations, and, as such, that it is not intended to replace the techniques[5,8−14] for obtaining diffusion coefficients of penetrants in the infinite dilution regime.

Acknowledgment. This work was granted access to the HPC resources of CCRT/CINES/IDRIS under Allocations 2009-095053 and 2010-095053 made by GENCI (Grand Equipement National de Calcul Intensif), France. The MUST cluster at the University of Savoie (France) is also acknowledged for its generous provision of computer time.

References and Notes

(1) Allen, M. P.; Tildesley, D. J. *Computer Simulation of Liquids*; Clarendon Press: Oxford, England, 1987.
(2) Yampolskii, Y.; Pinnau, I.; Freeman, B. D. *Materials Science of Membranes*; John Wiley & Sons Ltd.: Chichester, U.K., 2006.
(3) Müller-Plathe, F. *Acta Polym.* **1994**, *45*, 259–293.
(4) Müller-Plathe, F.; Rogers, S. C.; Van Gunsteren, W. F. *Chem. Phys. Lett.* **1992**, *199*, 237–243.
(5) Gusev, A. A.; Müller-Plathe, F.; Van Gunsteren, W. F.; Suter, U. W. *Adv. Polym. Sci.* **1994**, *116*, 207–247.
(6) Thran, A.; Kroll, G.; Faupel, F. *J. Polym. Sci., Part B: Polym. Phys.* **1999**, *37*, 3344–3358.
(7) Alentiev, A. Y.; Loza, K. A.; Yampolskii, Y. P. *J. Membr. Sci.* **2000**, *167*, 91–106.
(8) Gusev, A. A.; Arizzi, S.; Suter, U. W.; Moll, D. J. *J. Chem. Phys.* **1993**, *99*, 2221–2227.
(9) Gusev, A. A.; Suter, U. W. *J. Chem. Phys.* **1993**, *99*, 2228–2234.
(10) Greenfield, M. L.; Theodorou, D. N. *Mol. Sim.* **1997**, *19*, 329–361.
(11) Greenfield, M. L.; Theodorou, D. N. *Macromolecules* **1998**, *31*, 7068–7090.
(12) Greenfield, M. L.; Theodorou, D. N. *Macromolecules* **2001**, *34*, 8541–8553.
(13) Karayiannis, N. C.; Mavrantzas, V. G.; Theodorou, D. N. *Chem. Eng. Sci.* **2001**, *56*, 2789–2801.
(14) Karayiannis, N. C.; Mavrantzas, V. G.; Theodorou, D. N. *Macromolecules* **2004**, *37*, 2978–2995.
(15) Neyertz, S.; Brown, D.; Pandiyan, S.; Van der Vegt, N. F. A. *Macromolecules* **2010**, *43*, 7813–7827.
(16) Brown, D. *The gmq User Manual Version 4: available at* http://www.lmops.univ-savoie.fr/brown/gmq.html, 2008.
(17) Humphrey, W.; Dalke, A.; Schulten, K. *J. Mol. Graphics* **1996**, *14*, 33–38.
(18) Marque, G.; Neyertz, S.; Verdu, J.; Prunier, V.; Brown, D. *Macromolecules* **2008**, *41*, 3349–3362.
(19) Pandiyan, S.; Brown, D.; Neyertz, S.; Van der Vegt, N. F. A. *Macromolecules* **2010**, *43*, 2605–2621.
(20) Costello, L. M.; Koros, W. J. *J. Polym. Sci., Part B: Polym. Phys.* **1995**, *33*, 135–146.
(21) Okamoto, K.-I.; Tanihara, N.; Watanabe, H.; Tanaka, K.; Kita, H.; Nakamura, A.; Kusuki, Y.; Nakagawa, K. *J. Polym. Sci., Part B: Polym. Phys.* **1992**, *30*, 1223–1231.
(22) Coleman, M. R.; Koros, W. J. *J. Membr. Sci.* **1990**, *50*, 285–297.
(23) Coleman, M. R.; Koros, W. J. *J. Polym. Sci., Part B: Polym. Phys.* **1994**, *32*, 1915–1926.
(24) Pandiyan, S.; Brown, D.; Van der Vegt, N. F. A.; Neyertz, S. *J. Polym. Sci., Part B: Polym. Phys.* **2009**, *47*, 1166–1180.
(25) Cheung, P. S. Y.; Powles, J. G. *Mol. Phys.* **1976**, *32*, 1383–1405.
(26) Razmus, D. M.; Hall, C. K. *AIChE J.* **1991**, *37*, 769–779.
(27) Waldman, M.; Hagler, A. T. *J. Comput. Chem.* **1993**, *14*, 1077–1084.